



ELSEVIER

Journal of Chromatography A, 779 (1997) 263–274

JOURNAL OF  
CHROMATOGRAPHY A

## Aspects of the elution order inversion by pressure changes in programmed-temperature gas chromatography

F.R. Gonzalez<sup>a,\*</sup>, A.M. Nardillo<sup>a,b</sup>

<sup>a</sup>Universidad Nacional de La Plata, Facultad de Ciencias Exactas, Div. Química Analítica, 47 esq.115, 1900 La Plata, Argentina

<sup>b</sup>CIDEPINT, 52 e/121 y 122, 1900 La Plata, Argentina

Received 13 November 1996; received in revised form 15 April 1997; accepted 21 April 1997

### Abstract

The phenomenon of elution order inversion in programmed-temperature gas chromatography, as a result of only changing the head pressure of the column while retaining the same temperature program, is known to be experimentally detectable. In this paper we analyze some theoretical aspects of this phenomenon. These aspects concern the dependence of the separation on the pressure program for a couple of analytes presenting a retention reversal in isothermal gas chromatography (GC). In the theoretical context, the reason why the pressure program will not have a uniform effect on the separation of all crossing-over couples from a mixture, and why it is not possible to obtain a simple correlation for the separation of a given couple under different pressure conditions is visualized. A complete simulation of the process is required to evaluate the effect of the chosen head pressure–temperature program on the separation of the solutes. © 1997 Elsevier Science B.V.

**Keywords:** Temperature programming; Elution order; Pressure programming

### 1. Introduction

The experimental conditions involved in the occurrence of peak elution order inversions, by applying different inlet pressures to the column ( $p_i$ ) while using the same temperature program, were reported by Pell and Gearhart [1]. The consequences were discussed, warning chromatographers to be careful in selecting flow conditions for the analysis of a complex mixture in programmed-temperature gas chromatography (PTGC). The theoretical interest in the effect is that it reflects the importance of the column head pressure function  $p_i(T)$  (the pressure

program) in affecting the relative retention, or the separation, for a pair of analytes during a temperature program.

We shall focus our study on a couple of solutes ( $x, y$ ) with different isothermal elution orders at two different temperatures. In isothermal GC the separation is governed by thermodynamics through the difference of the capacity factors  $k$ :

$$t_{Ry} - t_{Rx} = t_M(k_y - k_x) \quad (1)$$

The coelution temperature  $T_{Ce}$  (i.e., when  $k_y = k_x$ ) is the temperature where the cross-over occurs, with further inversion in the elution order. For example, if  $k_x < k_y$  when  $T < T_{Ce}$ , and when  $k_x > k_y$  for  $T_{Ce} < T$ , the elution order is inverted. The fluid dynamics, reflected in the gas hold-up parameter  $t_M$ , have no

\*Corresponding author.

influence on the elution order of the peaks<sup>1</sup>. In contrast, in programmed-pressure and temperature gas chromatography (PPTGC) the retention differences within a couple of peaks are controlled by both the fluid dynamics and the thermodynamics [3,4]. This cooperative relationship between factors enables the inversion by affecting only the flow [i.e., changing  $p_i(T)$  or  $t_M(T)$ ] while preserving the parameters of the temperature program: the initial temperature  $T_0$  and the heating rate  $r_T$ .

The objective of this paper is to introduce a theoretical description of the problem which allows a visualization of the influence of the different variables causing this phenomenon. The theoretical description is employed to point out those aspects of general interest, concerning the effect of  $p_i(T)$  on the separation of any pair of solutes.

## 2. Experimental

Experiments were performed with Hewlett-Packard 5880A and 5890 Series II Plus chromatographs. The latter equipment contains an electronic pressure control device (EPC), governed by a microprocessor, allowing three types of  $p_i$  control. Two columns were used: an AT-1 (Alltech, IL, USA) 30 m×0.25 mm I.D. with a 0.25 μm poly(dimethylsiloxane) film, and a Hewlett Packard (25 m×0.25 mm I.D., 0.25 μm), coated with Carbowax 20M. The solutes were injected as vapors using gas-tight syringes. The applied split ratios ranged from 40 to 100:1, using nitrogen or hydrogen as carrier gases. The injection volumes were selected such that significant signals were obtained at the lowest attenuation. Flame ionization detection (FID) was used, employing methane as the unretained solute for  $t_M$  determination. The head pressure was read directly from the chromatograph's display when high values were required, otherwise using a 150 cm long mercury column manometer. Head pressure evolution was controlled through measured  $t_M$  values, as indicated in Section 3.3. The ambient pressure was measured by means of a Fortin barometer.

<sup>1</sup> Nevertheless, for non-ideal behavior of the vapor phase a pressure effect on  $k$  is expected that could, in principle, modify the separation in isothermal GC [2].

Curve fitting by non-linear regression of the experimental isothermal retention data was performed with Sigma Plot software (Jandel Scientific, CA, USA) which applies the Marquardt–Levenberg iterative algorithm.

## 3. General

### 3.1. Condition of coelution in programmed-pressure and temperature gas chromatography (PPTGC)

The integration of the equation of peak motion in a single ramp linear temperature program leads to the general expression, valid for any pressure program [5]:

$$1 = \frac{1}{r_T} \int_{T_0}^{T_R} \frac{dT}{t_R(T)} = \frac{1}{r_T} \int_{T_0}^{T_R} \frac{dT}{t_M(T)[1+k(T)]} \quad (2)$$

where  $t_R(T)$  and  $t_M(T)$  are, respectively, the isothermal retention time and the isothermal gas hold-up time at temperature  $T$ .  $T_R$  is the retention temperature. The isothermal gas hold-up function, for capillary or packed columns, is given by [3,4]:

$$t_M(T) = C_t^{-1} T^N \frac{[p_i^3(T) - p_0^3]}{[p_i^2(T) - p_0^2]^2} \quad (3)$$

where  $C_t^{-1}$  is a constant for the column–carrier gas combination that can be easily determined experimentally [3,4].  $N$  is the exponent of the power law describing the temperature dependence of the carrier gas viscosity [6].

Taking the difference of Eq. (2) for two crossing-over solutes ( $x, y$ ), imposing the condition of coelution, yields:

$$\int_{T_0}^{T_{\text{CePT}}} \frac{[t_{Ry}(T) - t_{Rx}(T)]}{t_{Ry}(T)t_{Rx}(T)} dT = C_t \int_{T_0}^{T_{\text{CePT}}} \frac{[p_i^2(T) - p_0^2]^2}{[p_i^3(T) - p_0^3]T^N} \times \left[ \frac{1}{[1+k_x(T)]} - \frac{1}{[1+k_y(T)]} \right] dT = 0 \quad (4)$$

$I_c(T)$  and  $I_t(T)$  are, respectively, the left and right integrands of Eq. (4).  $T_{\text{CePT}}$  is the coelution temperature in an appropriate pressure–temperature program. This equation will be satisfied whenever the area under the curve  $I_c(T)$  [or  $I_t(T)$ ] vs.  $T$  is zero. For example, if  $k_x < k_y$  when  $T < T_{\text{Ce}}$ , then the positive area in the interval  $[T_0, T_{\text{Ce}}]$  has to be equal to the negative area in the interval  $[T_{\text{Ce}}, T_{\text{CePT}}]$ , in order to comply with Eq. (4). Throughout this paper we shall preserve this convention for subindexes  $x$  and  $y$  and the latter will be invariably an  $n$ -alkane in the examples chosen to illustrate the theoretical notions.

In addition to Eq. (4), the retention equation for each solute must be obtained individually, making  $T_{\text{R}}$  equal to  $T_{\text{CePT}}$ :

$$C_t^{-1} = \frac{1}{r_T} \int_{T_0}^{T_{\text{R}}} \frac{[p_i^2(T) - p_0^2]^2 dT}{[p_i^3(T) - p_0^3] T^N [1 + k_x(T)]} \quad (5)$$

Eq. (5), which is derived from the combination of Eqs. (2) and (3), was compared in a related work [4] against experimental retention data by applying different head-pressure programs  $p_i(T)$ .

An essential difference exists between the isothermal coelution temperature  $T_{\text{Ce}}$  and the programmed temperature  $T_{\text{CePT}}$ . The first is a unique thermodynamic parameter, as there is only one temperature matching  $k_x(T_{\text{Ce}}) = k_y(T_{\text{Ce}})$ . The second depends upon the selected program parameters: initial temperature, heat rate and the pressure program  $p_i(T)$ ; there are as many  $T_{\text{CePT}}$  values as the number of times Eqs. (4) and (5) can be simultaneously satisfied.

The integrand  $I_c(T)$  in Eq. (4), can not be directly experimentally evaluated, and only requires isothermal retention times taken at different temperatures. It concerns no other theoretical notion than assimilation of the programmed-temperature process to a summation of sequential isothermal states. This is the most basic hypothesis of the PTGC theory. In contrast, the integrand  $I_t(T)$  involves further theoretical reductionisms [4]. Calculation of the latter demands knowledge of the  $p_i(T)$  and  $k(T)$  functions. The head-pressure function is accessible for most types of flow control devices with chromatographic applicability [3]. The temperature dependence of the capacity factor deserves some examination.

### 3.2. The $k(T)$ function

The general thermodynamic relationship for the GLC process may be written conveniently as:

$$\begin{aligned} \ln k(T) &= -\frac{\Delta G(T)}{RT} - \ln \beta \\ &= \left( \frac{\Delta S(T)}{R} - \ln \beta \right) - \frac{\Delta H(T)}{RT} \end{aligned} \quad (6)$$

where  $\Delta H(T)$  and  $\Delta S(T)$  functions are the partial molar enthalpy and entropy of solution, respectively. The term containing the phase ratio  $\beta$  of the column was bracketed adjoining the entropic term in order to point out the fact that they cannot be determined independently by the procedures described in this section. The pressure dependence of the thermodynamic functions [2] was neglected in the expression, assuming ideal behavior for the vapor phase. The experimental determination of  $k$  is obtained from the isothermal retention and gas hold-up as:  $k^{\text{exp.}}(T) = [t_{\text{R}}(T)/t_{\text{M}}(T)] - 1$ .

Traditionally, the numerical simulation of the PTGC process has been carried out determining  $k(T)$  by means of a linear regression of isothermal retention data against the reciprocal absolute temperature [4,7–9]. The linear regression of experimental data to Eq. (6) neglects the temperature dependence of the enthalpic and entropic functions, assuming them as constant parameters. Despite this limitation, the approximation has proven to be useful, yielding good accuracy in the final predicted retention times for weakly and medium retained solutes. However, this is a poor descriptor of  $k(T)$  in a broad temperature interval and its application to strongly retained solutes, in a program started at low initial temperatures, is expected to generate discrete errors. The incidence of the linear approximation on the errors of predicted retention times, through the resolution of Eq. (2), was evaluated by Vezzani et al. [10]. The same has been done for empirical expressions that yield a more precise fitting of the experimental data to the proposed  $k(T)$  functions [10]. Here, we shall adopt the procedures of Clarke and Glew [11] and Castells et al. [12] for describing  $k(T)$ . This has the advantage of being thermodynamically rigorous, thus preserving the physical meaning of all the parameters present in the derivations. It assumes that the stan-

standard enthalpy change in a given process at temperature  $T$ ,  $\Delta H(T)$ , can be expressed as a Taylor's series expansion on the value  $\Delta H(T^0)$ , at some reference temperature  $T^0$ . The standard free energy change of the process, writing only the first three terms of the series, renders:

$$-\frac{\Delta G(T)}{T} = -\frac{\Delta G(T^0)}{T^0} + \Delta H(T^0) \left[ \frac{1}{T^0} - \frac{1}{T} \right] + \Delta C_p(T^0) \left[ \frac{T^0}{T} + \ln \left( \frac{T}{T^0} \right) \right] + \dots \quad (7)$$

where  $\Delta C_p$  is the change of the isobaric molar heat capacity in the standard states. Applying this to the chromatographic process, using partial molar quantities, leads to the following relationships for  $k(T)$ , being a special case of the more general Eq. (6):

$$\ln k(T) = a + \frac{b}{T} + c \ln T \quad (8)$$

where

$$\frac{\Delta C_p}{R} = c \quad (9)$$

$$\begin{aligned} \frac{\Delta H(T)}{R} &= -b + cT \\ &= \frac{\Delta H(T^0)}{R} + \frac{\Delta C_p}{R}(T - T^0) \end{aligned} \quad (10)$$

$$\frac{\Delta S(T)}{R} - \ln \beta = a + c(1 + \ln T) \quad (11)$$

$$\frac{\Delta S(T)}{R} = \frac{\Delta S(T^0)}{R} + \frac{\Delta C_p}{R} \ln(T/T^0) \quad (12)$$

As shown, taking only the first three members of the series means that the change in the heat capacity is assumed to be constant with temperature. These equations also imply ideal behavior for the vapor phase, having the same mentioned limitation as Eq. (6) [2]. If only the first two members of the series are retained, the expression of  $k(T)$  is reduced to the linear regression of Eq. (6). Taking the first four terms accounts for the temperature dependence of  $\Delta C_p$ , which is known to be a very small contribution [12].

Fig. 1a presents experimental values of  $\ln [(t_R /$

$t_M) - 1]$  (triangles) and the regression curves by using Eq. (8) (lines) for the crossing couples 2,5-dimethylpyridine/*n*-tridecane and 3,5-dimethylpyridine/*n*-tetradecane on the Carbowax column, as an example of a polar system. Fig. 1b is an example for the non-polar case, using the silicone column and the *sec.*-butylbenzene/*n*-decane pair. As illustrated, the non-linear regression accounts for the curvature of the  $\ln k$  vs.  $(1/T)$  plot, providing a precise curve fitting for the experimental data along the whole temperature interval of almost 200 K. Parameters  $a$ ,  $b$  and  $c$  for the thermodynamic functions of Eqs. (8)–(11) are indicated in Table 1, columns 4 to 6.

The values for  $\Delta H/R$  and  $(\Delta S/R) - \ln \beta$  obtained from the linear regression of the same isothermal retention data are reported in Table 1, columns 2 and 3. The seventh column indicates the temperature at which  $\Delta H(T)$  and  $\Delta S(T)$  functions from Eqs. (10) and (11) meet the values rendered by the linear approximation. The latter would be an evaluation at the temperature corresponding to the medium value of the  $1/T$  interval, shown in column 8. In principle,  $1/T$  should not coincide exactly with the temperature of agreement between linear and non-linear regressions because the rate of change in the slope of a curve from Fig. 1 is not constant (the second derivative of  $\ln k$  with respect to  $1/T$  depends on  $T$ ; for example, from the derivation of Eq. (8) we obtain:  $\partial^2 \ln k / \partial (1/T)^2 = cT^2$ ). However, what can be observed is that this effect is negligible, and in general we can state that the linear regression only provides the values of  $\Delta H(T)$  and  $\Delta S(T)$  functions at the temperature of  $1/T$ .

The fact described above does not mean that gross errors could be avoided by using the linear approximation. According to Eq. (10), the absolute value of  $\Delta H(T)/R$  decreases with  $T$  at a rate of  $\Delta C_p/R$ , which has an order of 10. For example, the value for *sec.*-butylbenzene at 230°C is 20% lower than that at 112°C. The same consideration can be formulated for  $(\Delta S(T)/R) - \ln \beta$  using Eq. (11).

The coelution temperature for a pair of solutes is given by the general condition:

$$T_{ce} = \left[ \frac{\Delta H_y - \Delta H_x}{\Delta S_y - \Delta S_x} \right]_{T_{ce}} \quad (13)$$

Note that this condition expresses an implicit

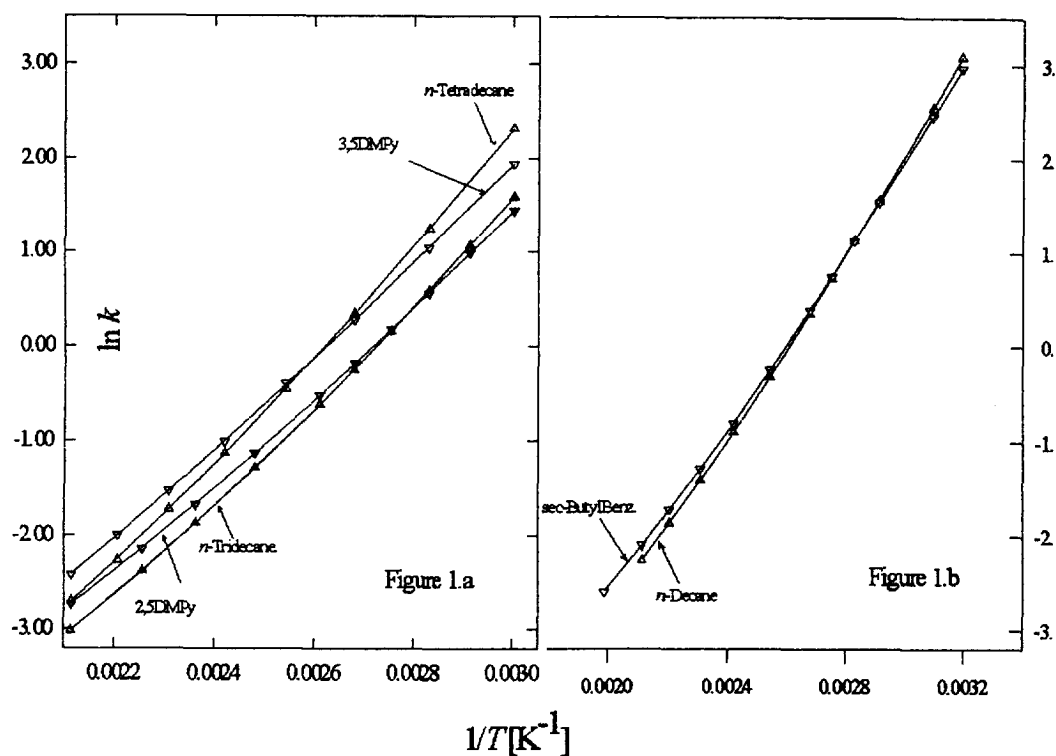


Fig. 1. Non-linear regression curves (Eq. (8)) for experimental  $k$  data. ( $\nabla$ ) for 2,5- and 3,5-dimethylpyridine (DMPy) and *sec*-butylbenzene ( $x$ ), ( $\Delta$ ) for the crossing  $n$ -alkane ( $y$ ). Filled lines are the regression curves.

Table 1  
Thermodynamic parameters from linear and non-linear regressions

Solute	Linear regression to Eq. (6)		Non-linear regression Eq. (8)				
	$-\Delta H/R$ (K)	$-[(\Delta S/R) - \ln \beta]$	$-a$	$b$ (K)	$c$	$T$	$T$ at $\bar{1}/\bar{T}$
<i>Carbowax column</i>							
2,5-DMPy	4713	12.78	69.160	7888.9	8.0766	120.1	117.8
<i>n</i> -Tridecane	5194	14.11	96.295	9824.3	11.7740	120.1	117.8
3,5-DMPy	4909	12.85	55.917	7344.5	6.1652	121.8	117.8
<i>n</i> -Tetradecane	5655	14.76	93.186	10 089.8	11.2270	121.8	117.8
<i>Silicone column</i>							
<i>sec</i> -Butylbenzene	4668	12.09	66.624	7691.3	7.8369	112.6	112.8
<i>n</i> -Decane	4903	12.76	76.739	8457.6	9.1910	113.6	112.8
Naphthalene	5106	12.28	43.040	6922.0	4.3756	142.0	147.8
<i>n</i> -Dodecane	5559	13.29	81.539	9601.6	9.7006	143.6	147.8

Columns 2 and 3: thermodynamic parameters obtained from the linear regression of Eq. (6). Columns 4 to 6: parameters obtained from the curve fitting of the experimental data to Eq. (8). Column 7: temperature at which  $\Delta H(T)/R$  and  $-[(\Delta S(T)/R) - \ln \beta]$  functions from Eqs. (10) and (11) agree with the linear approximation. Column 8: temperature corresponding to the medium value of the  $1/T$  interval.

function for  $T_{Ce}$ . According to the linear regression  $T_{Ce}$  is determined by:

$$T_{Ce} = \frac{(\Delta H_y - \Delta H_x)}{R \left[ \left( \frac{\Delta S_y}{R} - \ln \beta \right) - \left( \frac{\Delta S_x}{R} - \ln \beta \right) \right]} \quad (14)$$

and according to the non-linear regression is determined by the solution of the implicit expression:

$$(a_x - a_y) + \frac{(b_x - b_y)}{T_{Ce}} + (c_x - c_y) \ln T_{Ce} = 0 \quad (15)$$

The coelution temperature calculated from the linear regression (Eq. (14)) will not differ significantly from the precise one calculated from Eq. (15) if the isothermal data used in the regression belongs to the surroundings of  $T_{Ce}$ , e.g., for *sec.*-butylbenzene/*n*-decane, both equations yield  $T_{Ce} = 351.2$  K.

### 3.3. The $t_M(T)$ function

A reliable evaluation of the head-pressure control performance during a chromatographic run can be obtained through the gas hold-up time  $t_M$ . This has also been used for indirect  $p_i$  determination [9], when using capillary columns. One important source of errors in GC stems from the existence of small head-pressure fluctuations, especially those produced during injection. In the case of the EPC device, the head depression generated by a small leakage during septum puncture will be rapidly compensated by the system. Sometimes this perturbation is not even perceptible by  $p_i$  electronic monitoring, but can be detected by the resultant gas hold-up. The high degree of confidence of the retention data, required for the determination of thermodynamic parameters, makes this evaluation unavoidable. Table 2, column 2 indicates the expected  $t_M$  values at each temperature for the constant  $p_i$  mode of flow control, calculated using Eq. (3). The expected  $t_M(T)$  function from Eq. (3) is represented in Fig. 2 by a filled line. The third column of Table 2 tabulates the averages of  $t_M$  from different chromatograms, obtained at each temperature for thermodynamic parameter determinations. These are represented as circles in Fig. 2. The filled line in the figure served as a smooth, continuous reference for detecting fluctuations of the inlet pressure during runs. The

Table 2

Calculated and experimental isothermal gas hold-up time under constant head pressure on the silicone column

$T$ (°C)	$t_M$ calc. (min)	$t_M$ exp. (min)
35	2.090	2.090
40	2.115	2.113
50	2.164	2.164
60	2.212	2.215
70	2.260	2.262
80	2.307	2.307
100	2.401	2.409
120	2.494	2.499
140	2.585	2.590
160	2.676	2.675
200	2.852	2.862
230	2.982	2.987

comparison indicates a high performance of the EPC in maintaining the preset inlet pressure with time, and withstanding rough temperature changes. Nevertheless, nothing can prevent the occurrence of an eventual transient head depression produced by a imperceptible “blow” (not a permanent leakage) during injection, invalidating the chromatogram.

## 4. The elution order inversion

Fig. 3a–c represent the experimental (circles) and theoretical (filled lines) integrands of Eq. (4), the isothermal separation functions. All the examples were taken in the constant head pressure mode of flow control. Fig. 1a,b show 2,5-dimethylpyridine/*n*-tridecane and 3,5-dimethylpyridine/*n*-tetradecane on the Carbowax column. Fig. 3c illustrates the behavior of the integrands for *sec.*-butylbenzene/*n*-decane on the silicone column, expressed as dimensionless quantities  $I^*$ , dividing  $I_e(T)$  and  $I_i(T)$  by the measured value of the constant  $C_t(p_i^2 - p_0^2)^2 / T_{Ce}^N (p_i^3 - p_0^3)$  ( $\text{min}^{-1}$ ). This was done with the aim of extending the utility of the figure, making the graph independent of the pressure conditions, noting that in the constant  $p_i$  mode the pressure factor can be taken out of the integral of Eq. (4). Although, changing the head pressure will not modify the profile of the dimensionless  $I^*$ , it certainly will affect the absolute value of the area on a

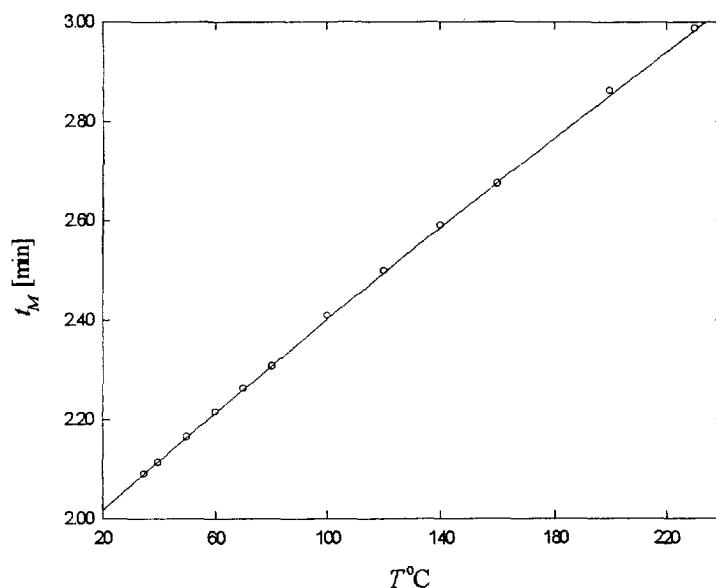


Fig. 2. Control curve for the isothermal gas hold-up at constant  $p_1$ . Filled line: theoretical control curve. Circles: experimental data on the silicone column, using  $N_2$  as carrier gas ( $N=0.725$ ). Column constant:  $C_1^{-1}=2.995 \text{ min kPa/K}^{0.725}$ .

dimensional basis. Therefore, if we pretend to compare what happens during the PTGC process under two different  $p_1$  conditions, using the constant pressure mode, the dimensionless representation is more convenient. The dimensionless abscissa is  $T^*=T/T_{C_c}$ .

The agreement between the experimental  $I_c(T)$  (circles) and the theoretical  $I_1(T)$  (filled line) observed in Fig. 3a–c was expected a priori, since  $k(T)$  and  $t_M(T)$  functions can be described accurately, as illustrated by Figs. 1 and 2. The dashed line in Fig. 3a represents the linear approximation to  $k(T)$ , showing that under certain circumstances the particular distribution of the errors may lead to a compensation, when computing a numerical estimate of the separation of such an approach. But we should be aware that this will not be always the case.

In isothermal GC optimal separations can be performed at the maximum and minimum  $I_c(T)$  values, noting that at these points the greatest separations ( $t_{R_y}-t_{R_x}$ ) are obtained in the shortest analysis time (lowest  $t_{R_y}t_{R_x}$  product). However these may not be “optimal” in practice, depending on the location of the coelution temperature  $T_{C_c}$  in relation to the interval that provides a reasonable analysis time. In Fig. 3a the maximum lies below the lowest

operating temperature for the Carbowax column (333 K).

So far we have a precise “static” description of the programmed temperature process, i.e., a description for the thermal evolution of the separation of  $x$ – $y$  as a sequence of isothermal states. The “dynamic” part of the description involves the integration of Eq. (4) or Eq. (5) assuming thermal equilibrium along the temperature program. There are basically three errors that could be committed in this part: (a) those associated to the discrepancy between the preset temperature program and the actual column temperature, including the errors generated by the thermal inertia of the oven, (b) those related to the departure from the thermal equilibrium condition at high heating rates [13,14] and (c) the error introduced by the numerical integration [5].

Formally, if the coelution condition in programmed temperature (Eq. (4)) is not satisfied, then the peaks  $x$ – $y$  become separated. If  $\int_{T_0}^{T_R} I_1(T) dT > 0$ ,  $x$  elutes before  $y$  and conversely if  $\int_{T_0}^{T_R} I_1(T) dT < 0$ . In other words, the order of elution depends on the ratio of the positive portion to the negative portion of the area covered by the programmed temperature process

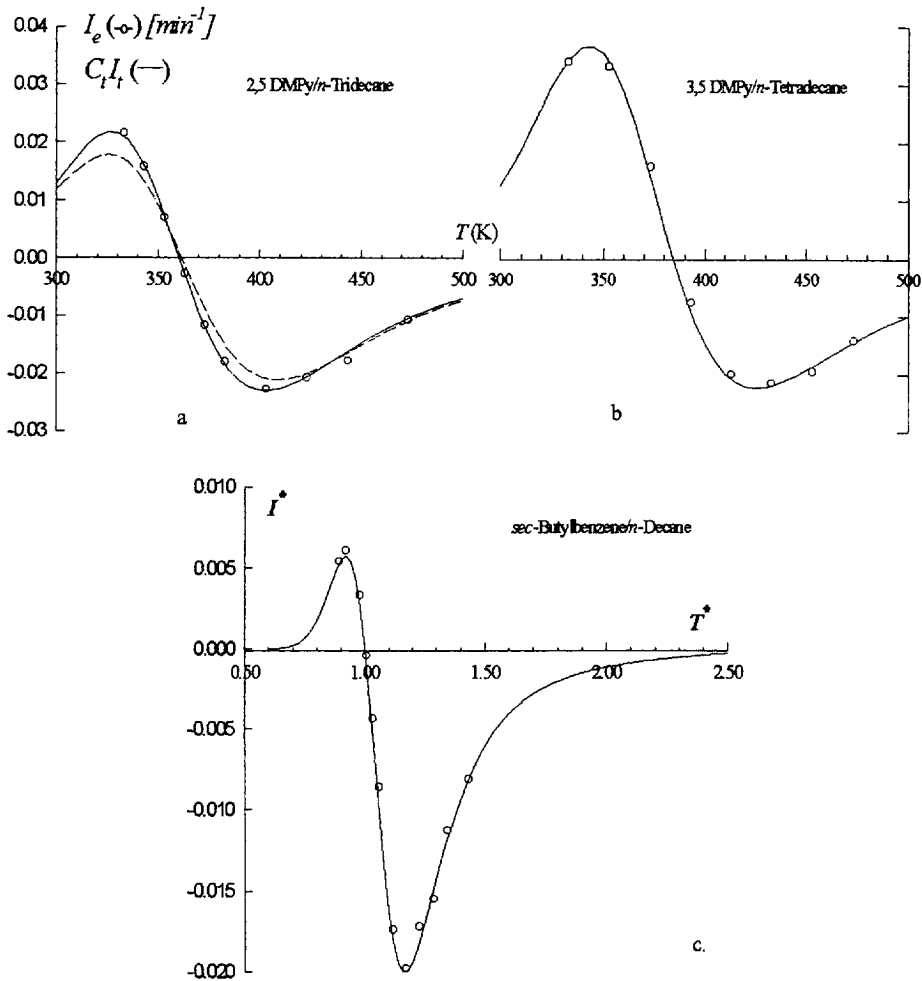


Fig. 3. Theoretical  $I_e(T)$  (filled line) and experimental  $I_e(T)$  (circles) separation functions. (a) Separation function for 2,5-dimethylpyridine/*n*-tridecane under constant head pressure,  $p_i=191.3$  kPa, carrier gas is  $\text{H}_2$  ( $N=0.68$ ). Column constant for the Carbowax column is  $C_i^{-1}=2.335$  min kPa/ $\text{K}^{0.68}$ . (b) *idem* for 3,5-dimethylpyridine/*n*-tetradecane. Dashed line is  $I_i$  using the linear approximation to Eq. (6). (c) A dimensionless representation for *sec*-butylbenzene/*n*-decane on the silicone column.

from  $T_0$  to  $T_R$ . According to the equation of retention (Eq. (5)), for a given  $x$ - $y$  system and fixed  $T_0$ , the length of the interval  $[T_0, T_R]$  depends on the heating rate  $r_T$  and the pressure program  $p_i(T)$ . The latter not only modifies the length of the scanned temperature interval, but also affects the shape of the curve (as is discussed in Section 5).

Fig. 4 presents, for sake of simplicity, only the theoretical curve of *sec*-butylbenzene/*n*-decane on the silicone column. The filled-in black part under the curve, located between  $T_0$  and  $T_{R1}$ , indicates the interval scanned by the temperature and pressure

programs specified by  $T_0=323.1$  K,  $r_T=5$  K/min,  $p_i=282.3$  kPa (abs.) = const.. The average retention temperature for the couple, under these conditions is  $T_{R1}$ . In this case the positive area is greater than the negative (almost imperceptible in the figure), consequently *sec*-butylbenzene ( $x$ ) elutes before *n*-decane ( $y$ ). The vertical line at  $T_{R2}$  marks the abscissa to which the elution of the pair is extended on average if  $p_i$  is reduced to 132.3 kPa (abs.), preserving the same temperature program. In this situation, the covered negative area (filled with vertical lines) becomes greater than the positive (black), and the



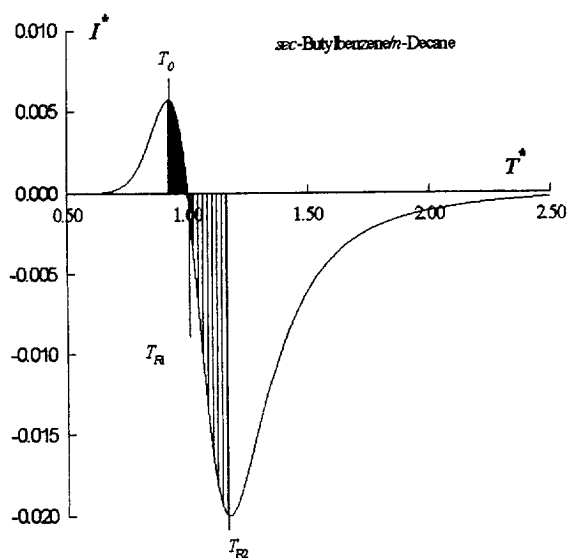


Fig. 4. Conditions for the elution order inversion of *sec*-butylbenzene/*n*-decane. Temperature program:  $T_0 = 323.1$  K and  $r_T = 5$  K/min. Pressure program 1 (elution at  $T_{R1}$ ):  $p_i = \text{const.} = 282.3$  kPa (abs). Covered area: surface filled in black. Pressure program 2 (elution at  $T_{R2}$ ):  $p_i = \text{const.} = 132.3$  kPa. Covered area: surface filled in black + surface filled with vertical lines. The coelution temperature is  $T_{C_c} = 351.2$  K.

inversion of the elution order is expected. Table 3 lists the observed differences of retention times, under the specified conditions, and the calculated differences obtained from the numerical solution of retention Eq. (5). To obtain a similar picture for the polar examples one should place the reported retention temperatures from Table 3 on the respective graph from Fig. 3. In the example of 3,5-DMPy/*n*-tetradecane the condition of coelution can be visualized.

The PT separation will be greater when the scanned area of a given sign, e.g., (+) is greater. When the (-) area begins to be covered by the temperature interval, the PT separation decreases until coelution is attained, i.e., when both areas reach the same absolute value. If a further extension of the scanned temperature interval, by reducing the inlet pressure, is contemplated, the likelihood of inverse separation increases.

We should remark on the fact that the numerical simulation through the solution of Eq. (2) or Eq. (5) is "blind" with respect to having some mental picture of how the separation will evolve by chang-

ing the chromatographic conditions. The representation of the  $I_c(T)$  curve permits us to visualize how the temperature retention interval should be situated in order to obtain a stipulated result for the separation of the couple.

## 5. Effects of pressure programming

The integrand  $I_i(T)$  is a function of the pressure program  $p_i(T)$  through the pressure factor  $\frac{[p_i^2(T) - p_0^2]^2}{[p_i^3 - p_0^3]}$ . If the pressure program is modified adequately, changes in the relative proportions of the positive and negative areas can be oriented to render a desired result. For example, Fig. 5 shows profiles of  $I_i(T)$  for naphthalene/*n*-dodecane on the silicone column, following two different pressure programs. As in the former example, experimental representation was avoided. Program A, symbolized by the filled line curve, is a constant  $p_i$  condition throughout the reduced temperature segment ( $p_i = 141.3$  kPa). Program B, represented by the dashed line, illustrates how the negative portion of the curve can be magnified by applying a specific programming design. This is a two step linear pressure program (LPP) defined by:

If  $T < T_{C_c}$ ,  $p_i = p_i^0 = 141.3$  kPa (abs.) = const; if  $T > T_{C_c}$ ,  $p_i = p_i^0 + (r_p/r_T)(T - T_{C_c})$ . The compression rate  $r_p$  in the figure is such that  $r_p/r_T$  is 2 kPa/K.

This is one aspect to be considered, as the relative proportions of the areas scanned by the  $[T_0, T_R]$  interval will define the order of elution and the separation in the case of crossing-over solutes. The other aspect to be considered is precisely how the program  $p_i(T)$  will affect the length of the interval for a fixed  $T_0$ . Fig. 6 shows the effect of increasing  $r_p$  of a single ramp LPP on the retention temperature of *n*-dodecane.

Increasing  $p_i$  for  $T > T_{C_c}$ , as in Program B of Fig. 5, will not have a perceptible net effect on incrementing the scanned negative area because the resultant magnification of  $I_i(T)$  is partially compensated by the reduction of the segment covered by  $[T_0, T_R]$ . But it must be observed that these opposite trends have different influences. The final result can

Table 3

Examples of observed and calculated elution order inversions and an example of observed and calculated condition of coelution<sup>a</sup>

Pair: 2,5-Dimethylpyridine (x)/ <i>n</i> -tridecane (y)		$p_i = 267.3$ kPa	$p_i = 131.9$ kPa
Temp. progr.: $T_0 = 333.1$ K, $r_T = 15$ K/min		$p_0 = 102.3$ kPa	$p_0 = 102.1$ kPa
$t_{R_x}$ (min) $_T$ (K)	exp.	1.910_361.8	6.047_423.8
	calc.	1.926_362.0	6.040_423.7
$t_{R_y}$ (min) $_T$ (K)	exp.	1.960_362.5	5.954_422.5
	calc.	1.987_363.0	5.973_422.7
$(t_{R_y} - t_{R_x})$ (s)	exp.	3.00	-5.58
	calc.	3.66	-4.02
Pair: <i>sec.</i> -Butylbenzene (x)/ <i>n</i> -decane (y)		$p_i = 282.3$ kPa	$p_i = 132.3$ kPa
Temp. progr.: $T_0 = 323.1$ K, $r_T = 5$ K/min		$p_0 = 101.3$ kPa	$p_0 = 101.3$ kPa
$t_{R_x}$ (min) $_T$ (K)	exp.	6.097_353.6	16.654_406.4
	calc.	6.099_353.6	16.660_406.4
$t_{R_y}$ (min) $_T$ (K)	exp.	6.206_354.6	16.519_405.7
	calc.	6.200_354.1	16.480_405.6
$(t_{R_y} - t_{R_x})$ (s)	exp.	6.54	-8.10
	calc.	6.06	-10.80
Pair: 3,5-Dimethylpyridine (x)/ <i>n</i> -tetradecane (y) <sup>a</sup>		$p_i = 266.7$ kPa	$p_i = 131.9$ kPa
Temp. progr.: $T_0 = 343.1$ K, $r_T = 15$ K/min		$p_0 = 102.2$ kPa	$p_0 = 102.1$ kPa
$t_{R_x}$ (min) $_T$ (K)	exp.	2.018_373.4	6.300_437.6
	calc.	2.033_373.6	6.300_437.6
$t_{R_y}$ (min) $_T$ (K)	exp.	2.154_375.5	6.300_437.6
	calc.	2.185_375.9	6.300_437.6
$(t_{R_y} - t_{R_x})$ (s)	exp.	8.16	0
	calc.	9.12	0

Calculated retention times were obtained solving the retention equation (Eq. (5)).

be only evaluated through the resolution of the retention Eq. (5).

## 6. Conclusions

From Fig. 3a–c some consequences of interest can be inferred. First, the fact that the pattern for the  $I_c(T)$  curve and the location of  $T_{C_e}$  are unique for each pair of crossing analytes, and the fact that this curve controls the separation, implies that the separation of all crossing couples of a mixture will evolve differently when a head-pressure and temperature program is applied. The net effect of the program on one couple will not be simply correlated to the result of another. Note that the relative proportions of the positive and negative areas are different for different couples, and the absolute values of the ordinates also differ. This point was mentioned in a previous paper [4]. Precisely, an

abnormal high value, with respect to non-crossing couples, of the parameter  $(t_{R_x} - t_{R_y})^{LLP} / (t_{R_x} - t_{R_y})^{CP}$  was detected for naphthalene/*n*-dodecane. LPP and CP indicate that the retention times were obtained using a linear pressure program and a constant head pressure, respectively. The same temperature program was applied to both modes. Second, we shall analyze now what can be inferred if we center our attention on a given couple. If we progressively change  $p_i$  between consecutive chromatograms, taken at the same temperature program, it is easy to see that the evolution of the separation will not adhere to a simple relationship, proving the complex nature of the  $I_c(T)$  function controlling this evolution. As different intervals of the curve are scanned, different separations are obtained. The same reasoning may be extended to the temperature program. Therefore, we may conclude that for a given couple, the effect on the separation from changing the temperature–pressure program will not be simply

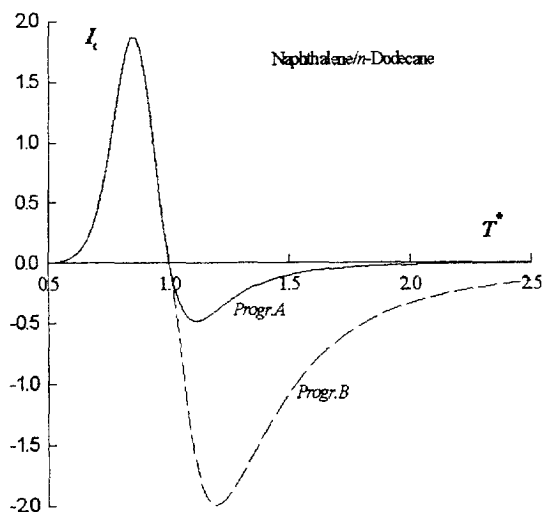


Fig. 5. Effects of pressure programming on  $I_i$  for naphthalene/*n*-dodecane. Filled line corresponds to pressure program A, defined by:  $p_i(T) = p_i^0 = 141.3$  kPa. Dashed line represents pressure program B, defined by: if  $T < T_{ce}$ , as for program A; if  $T > T_{ce}$ ,  $p_i(T)$ , silicone column. Only the abscissa is dimensionless. The coelution temperature is  $T_{ce} = 448.5$  K.

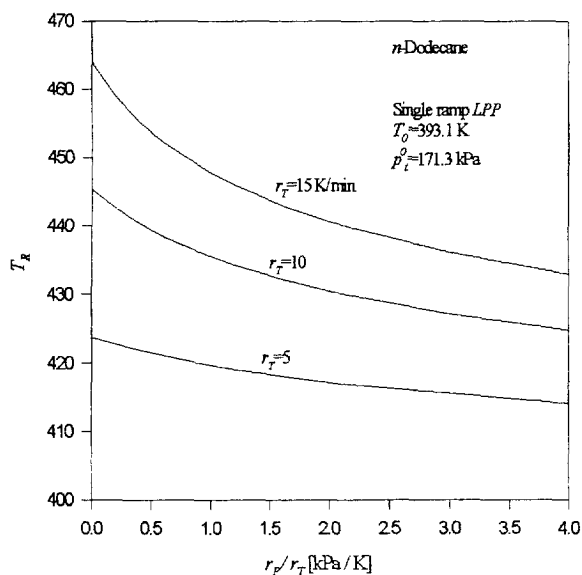


Fig. 6. Effect of pressure programming on the retention temperature of *n*-dodecane. Conditions: single ramp linear pressure program,  $T_0 = 393.1$  K, initial head pressure  $p_i^0 = 171.3$  kPa (abs.),  $p_i(T) = p_i^0 + (r_p/r_T)(T - T_0)$ , silicone column.

correlated to a reference condition. Again, the complex nature of the controlling  $I_e(T)$  will deprive us of finding simple retention relationships for the separation determined under different conditions.

Thirdly, even if the pressure and temperature program are standardized, the separation would not be the same if columns with different  $C_i^{-1}$  constants are used (of course, considering the same stationary phase). This results from the fact that the scanned temperature interval depends on this constant (implicit in Eq. (5)). So the geometric parameters of the column contained in this constant will also influence the separation.

The analysis of the relationship between the profile of the separation function  $I_i(T)$  or  $I_e(T)$  and the covered temperature interval  $[T_0, T_R]$  permits us not only to postulate an explanation for the elution order inversion phenomenon, but also to provide an appropriate framework for studying some factors influencing the relative retention of the solutes. For example, it explains why general correlations cannot be found between separations under different pressure programs when complex mixtures are analyzed, as was reported in a previous work [4]. It also shows that a uniform effect on the PT separation of the solutes can be expected, from changing the head pressure (in the CP mode), when  $I_e(T)$  is a constant parallel to the abscissa. This is a particular situation for non-crossing solutes.

Finally it should be concluded that the behavior of the separation of crossing solutes in PTGC is so complex that the only way to analyze the particular response to a change in the temperature–pressure program can be realized through the complete simulation of the chromatographic process.

The obvious implications on programmed-temperature retention index research, from the present report, will be discussed in a forthcoming paper.

## References

- [1] R.J. Pell, H.L. Gearhart, J. High Resolut. Chromatogr. 10 (1987) 388.
- [2] V.G. Berezkin, A.A. Korolev, I. Malyvkova, J. Microcol. Sep. 8 (1996) 389.
- [3] F.R. Gonzalez, A.M. Nardillo, J. Chromatogr. A 757 (1997) 97.

- [4] F.R. Gonzalez, A.M. Nardillo, *J. Chromatogr. A* 757 (1997) 109.
- [5] F.R. Gonzalez, A.M. Nardillo, *J. Chromatogr. A* 766 (1997) 147.
- [6] L.S. Ettre, *Chromatographia* 18 (1984) 243.
- [7] E.V. Dose, *Anal. Chem.* 59 (1987) 2414.
- [8] D.E. Bautz, J.W. Dolan, I.R. Snyder, *J. Chromatogr.* 541 (1991) 1.
- [9] H. Snijders, H.G. Janssen, C. Cramers, *J. Chromatogr. A* 718 (1995) 339.
- [10] S. Vezzani, P. Moretti, G. Castello, *J. Chromatogr. A* 677 (1994) 331.
- [11] E.C. Clarke, D.N. Glew, *Trans. Faraday Soc.* 62 (1966) 539.
- [12] R.C. Castells, E.L. Arancibia, A.M. Nardillo, *J. Chromatogr.* 504 (1990) 45.
- [13] P.Y. Shrotri, A. Mokashi, D. Mukesh, *J. Chromatogr.* 387 (1987) 399.
- [14] J.R. Conder, *J. Chromatogr.* 248 (1982) 1.